Contract No:

This document was prepared in conjunction with work accomplished under Contract No. 89303321CEM000080 with the U.S. Department of Energy (DOE) Office of Environmental Management (EM).

Disclaimer:

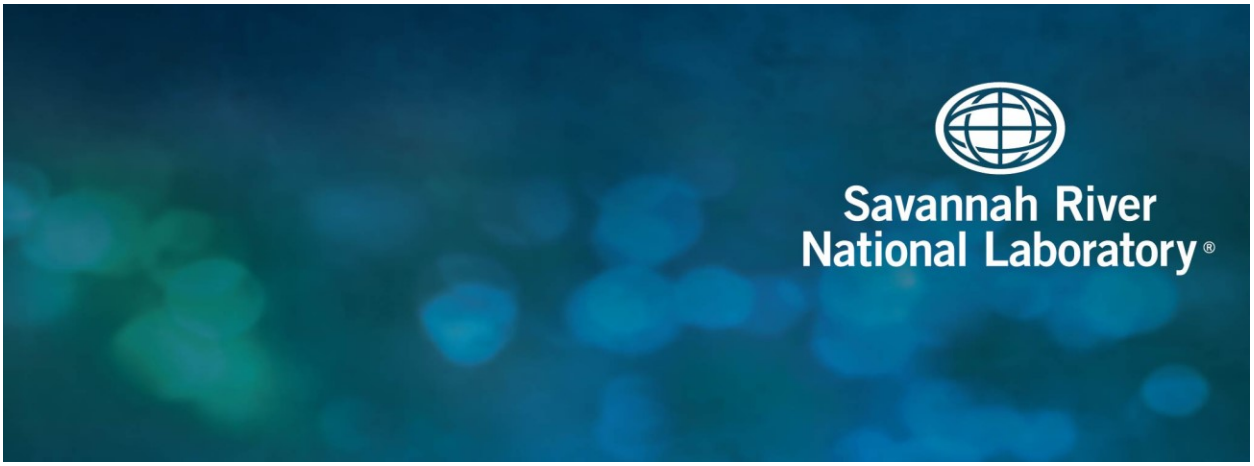

A U.S. DEPARTMENT OF ENERGY NATIONAL LAB • SAVANNAH RIVER SITE • AIKEN, SC • USA

Thermal Calculations to Determine Maximum Zircaloy Temperatures During Reactor Operations for Campaign 1 Fuel Assemblies

J. P. Folk

C. D. Skinner

May 2023

SRNL-STI-2023-00120, Revision 0

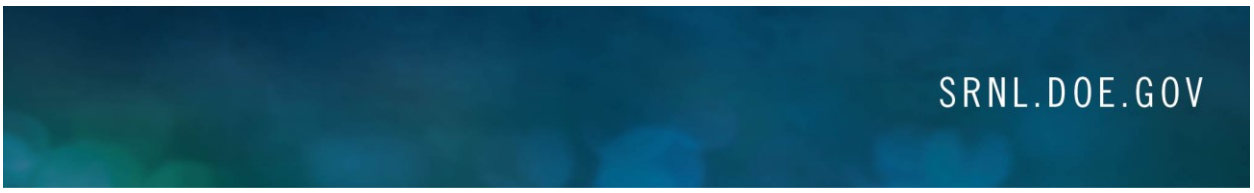

DISCLAIMER

Printed in the United States of America

Prepared for
U.S. Department of Energy

SRNL-STI-2023-00120
Revision 0

Keywords: *COMSOL, Fuel Assemblies, Thermal Calculation, Zircaloy*

Retention: *Permanent*

Thermal Calculations to Determine Maximum Zircaloy Temperatures During Reactor Operations for Campaign 1 Fuel Assemblies.

J. P. Folk
C. D. Skinner

May 2023

Savannah River National Laboratory is operated by Battelle Savannah River Alliance for the U.S. Department of Energy under Contract No. 89303321CEM000080.

REVIEWS AND APPROVALS

AUTHORS:

_____
J. P. Folk, Mechanical System & Custom Development Date

_____
C. D. Skinner, Engineering, Pressurized System and E&I Date

TECHNICAL REVIEW:

_____
J. E. Laurinat, Advanced Modeling & Simulation Date

APPROVAL:

_____
T. T. Truong, Separation Sciences & Engineering Date

_____
M. J. Mahoney, Manager Date
Mechanical System & Custom Development

_____
J. C. Kinney, Manager Date
Advanced Engineering

_____
A. M. Hudlow, Manager Date
Material Disposition Engineering

TABLE OF CONTENTS

LIST OF TABLES

LIST OF FIGURES

LIST OF ABBREVIATIONS

CHF	Critical Heat Flux
CVTR	Carolinas-Virginia Tube Reactor
DNB	Departure From Nucleate Boiling
EBWR	Experimental Boiling Water Reactor
HWCTR	Heavy Water Components Test Reactor
IAEA	International Atomic Energy Agency
NASNF	Non-Aluminum Spent Nuclear Fuel
SEP	Software Evaluation Package
SOT	Segmented Oxide Tube
SPRO	SRS P and R Production Reactors
SQAP	Software Quality Assurance Program
SRNL	Savannah River National Laboratory
SRS-R	Savannah River Site R-Reactor
STP	Software Test Plan
U	Uranium
UZr	Uranium-Zirconium
Zr2	Zircaloy-2
Zr4	Zircaloy-4

1. Introduction

The H-Canyon Facility plans on processing bundles from Non-Aluminum Spent Nuclear Fuel (NASNF) Risk Group 1 (UO_2 core fuels). Uranium-zirconium (UZr) alloys and zirconium clad UO_2 fuel containing UZr intermetallic compound have the potential to cause explosions during dissolution. UZr intermetallic typically only forms when uranium and zirconium (or zirconium alloy) cladding are in contact at high temperatures [1]. Thermal modeling was performed to determine the maximum cladding temperature for Campaign 1 Zircoloy cladded fuel assembles during reactor operation to help determine if the UZr intermetallic compound could have formed during reactor operations. The temperature of 350°C was chosen as a conservative minimum value for the possible formation of intermetallic UZr compound [2]. The modeling approach, inputs, and results are outlined in this document.

2. Thermal Modeling Process

2.1. Fuel Assembly Information

This document focuses on the 69 fuel bundles in NASNF Campaign 1 [2]. A simplified list is shown in Table 2-1. The table lists the reactor in which each fuel assembly was used and the relevant Appendix A document with detailed descriptions of the assembly. The fuel rods in Campaign 1 are from the following reactors: Carolinas-Virginia Tube Reactor (CVTR), Experimental Boiling Water Reactor (EBWR), Heavy Water Components Test Reactor (HWCTR), and Savannah River Site R-Reactor (SRS-R).

Prior to performing cladding temperature calculations, a subset of assemblies with the highest heat generation rates were identified from each Appendix A for analysis. The most conservative cases were chosen to bound the calculations and reduce the number of fuel assemblies requiring analysis. Only one CVTR assembly described by CVTR-001 Appendix A was analyzed, using the maximum power provided in “Design, Fabrication, and Operation of the CVTR High Power, High-Burnup Test Assemblies” [3]. A similar process was applied to the list of EBWR fuel assemblies. The assembly with the highest heat generation rate was analyzed from each of EBWR-002, EBWR-004, and EBWR-009 Appendix A files [4-6]. These values were found in a memo by Vinson [7]. Rods described by EBWR-001 Appendix A were not considered since the cladding on those rods is made of stainless steel and therefore there is no concern of UZr intermetallic formation. There is a large difference in rod diameters for fuel described in SOT-001 Appendix A, so the assembly with the highest heat generation rate and another assembly with a different rod diameter were analyzed [8]. The fuel assembly with the largest heat generation rate from SPRO-001 Appendix A was analyzed [9]. HWCTR-002 fuel is similar to HWCTR-004 fuel except for containing less than half as much U-235. Because HWCTR-004 establishes a bounding case, HWCTR-002 fuel was not analyzed. The condensed table of the analyzed fuel assemblies is shown in Table 2-1.

Table 2-1. Analyzed Fuel in Campaign 1

Reactor	Appendix A
CVTR	DOESRAAD-CVTR-001 [10]
EBWR	DOESRAAD-EBWR-002 [4]
EBWR	DOESRAAD-EBWR-009 [6]
EBWR	DOESRAAD-EBWR-004 [5]
HWCTR	DOESRAAD-HWCTR-004 [11]
HWCTR	DOESRAAD-SOT-001, Rev. 2 [8]
SRS-R	DOESRAAD-SPRO-001 [9]

2.2. Thermal Modeling Approach and Assumptions

COMSOL Multiphysics 6.0 was used for this analysis. COMSOL has been approved for use on heat transfer calculations through the Savannah River National Laboratory (SRNL) software quality approval process and is a Level B software. The document numbers for the Software Quality Assurance Program (SQAP), Software Evaluation Package (SEP), and Software Test Program (STP) are provided in the reference section [12-14]. Two dimensional (2D) models of individual fuel rods were used for this analysis. It was determined that it is not necessary to model the entire assembly, but instead to use the most conservative scenario. The most conservative case, assuming even fuel composition for rods within an assembly, would be an interior rod. Heat generated within the fuel element is transferred through the cladding and is lost through radiation and convection on the surface of the cladding. Radiative heat loss from the surface of the rod is not applied to the model, because an interior rod would receive heat through radiation from surrounding rods. It is assumed that this radiative heating from surrounding rods offsets heat loss through radiation. This is a conservative assumption because a portion of the radiative heat from each rod would be lost to the surrounding reactor components and could not all be transferred to other rods. It is also assumed that the fuel is in contact with the cladding. There is a helium gap in some fuel rod designs, but fuel may not have remained centered and fuel expansion likely occurred during reactor operations. This is modeled using the Thermal Contact condition in COMSOL. This assumes contact between two solids with interstitial gas to account for the helium and is further explained in the Inputs section of this document. This approach is used for modeling all of the fuel assemblies, with the major differences being: diameter and shape of fuel, diameter and shape of cladding, heat generation rate, reactor coolant type, coolant pressure, coolant temperature, and whether standard convection or nucleate boiling occurs on the surface of the fuel rods.

Another important assumption is that Departure from Nucleate Boiling (DNB) did not occur during BWR reactor operations. When this occurs a layer of steam forms on the surface of the fuel rods, resulting in poor heat transfer to the water and substantially higher cladding temperatures. The occurrence of DNB is determined by comparing the actual heat flux to the Critical Heat Flux (CHF). The Groeneveld correlation and Groeneveld lookup table data [15, 16] were used for calculating the CHF for EBWR-004 rods, since these had the highest heat flux. This calculation is shown in Appendix 2. It was determined that the actual heat flux was much lower than the CHF, so DNB did not occur during reactor operations.

2.3. Input Parameters

2.3.1. Material Properties:

The material properties for the Zircoloy cladding and uranium dioxide fuel are found in Table 2-2. Since the fuel rods have a wide range of fuel temperatures, the uranium dioxide properties are given at various temperatures.

Table 2-2. Material Properties of Solids Used in Models

Material	Thermal Conductivity (W/(m*K))	Density (kg/m^3)	Heat Capacity (J/(kg*K))	Young's Modulus (GPa)	Poisson's Ratio
Zircoloy (Zr2)	$(0.138-3.9x10^{-5}T+ 1.184x10^{-7}T^2) x100$ [17]	6560 [18]	285 [18]	99 [18]	0.37 [18]
Zircaloy (Zr4)	$(0.113+2.25x10^{-5}T+ 0.725x10^{-8}T^2) x100$ [17]	6560 [18]	285 [18]	99 [18]	0.37 [18]
Uranium Dioxide 500 °C	4.28 [19]	10800 [19]	303 [19]	219 [20]	0.319 [20]
Uranium Dioxide 850 °C	3.13 [19]	10680 [19]	315 [19]	219 [20]	0.319 [20]
Uranium Dioxide 2800 °C	2.93 [19]	9596 [19]	766 [19]	219 [20]	0.319 [20]

The properties of the helium, steam, water, and heavy water are found in Table 2-3. Many of these values are predefined for use within COMSOL, but the heavy water material properties were found in literature and input into COMSOL during modeling.

Table 2-3. Material Properties of Gases and Liquids Used in Models

Material	Thermal Conductivity (W/(m*K)	Density (kg/m^3)	Heat Capacity (J/(kg*K))	Dynamic Viscosity (Pa*s)	Ratio of Specific Heats	Specific Gas Constant	Mean Molar Mass (kg/mol)
Helium	COMSOL Predefined Value	COMSOL Predefined Value	COMSOL Predefined Value	COMSOL Predefined Value	COMSOL Predefined Value	COMSOL Predefined Value	COMSOL Predefined Value
Steam	COMSOL Predefined Value	COMSOL Predefined Value	COMSOL Predefined Value	COMSOL Predefined Value	COMSOL Predefined Value	COMSOL Predefined Value	COMSOL Predefined Value
Water	COMSOL Predefined Value	COMSOL Predefined Value	COMSOL Predefined Value	COMSOL Predefined Value	COMSOL Predefined Value	N/A	N/A
Heavy Water (1000psig and 240C)	0.556 [21]	902.6 [22]	4540 [23]	0.0001* [22, 24]	N/A	N/A	N/A
Heavy Water (5 psig and 115C)	0.634 [25]	1052 [26]	4180 [23]	0.00028 [27]	N/A	N/A	N/A

*calculated using kinematic viscosity [24] and density [22]

2.3.2.Geometry:

All fuel elements being examined are either rods or tubes. Since it is assumed that the fuel expands and is in contact with the cladding, the gap is modeled using the Thermal Contact heat transfer method. The dimensions for the rod-shaped fuel rods can be found in Table 2-4. The dimensions for the tube-shaped fuel rods can be found in Table 2-5.

Table 2-4. Dimensions of Rod-Shaped Fuel Rods

Reactor	Appendix A	Radius of Fuel (in)	Outer Radius of Cladding (in)	Length of Fuel (in)
CVTR	DOESRAAD-CVTR-001	0.218 [10]	0.244 [10]	95.4 [10]
EBWR	DOESRAAD-EBWR-002	0.186 [4]	0.213 [4]	48 [4]
EBWR	DOESRAAD-EBWR-009	0.188 [6]	0.213[6]	48 [6]
EBWR	DOESRAAD-EBWR-004	0.186 [5]	0.213 [5]	48 [5]

Table 2-5. Dimensions of Tube-Shaped Fuel Rods

Reactor	Appendix A	Assembly ID	Inner Radius of Cladding (in)	Inner Radius of Fuel (in)	Outer Radius of Fuel (in)	Outer Radius of Cladding (in)	Length of Fuel (in)
HWCTR	DOESRAAD-HWCTR-004	OT1-7	0.735 [11]	0.765 [11]	1.00 [11]	1.03 [11]	111.25 [11]
HWCTR	DOESRAAD-SOT-001, REV. 2	SOT 8-2	1.49 [8]	1.52 [8]	1.80 [8]	1.83 [8]	69.125* [8]
		SOT 1-3	0.735 [8]	0.765 [8]	1.00 [8]	1.03 [8]	78.75* [8]
SRS-R	DOESRAAD-SPRO-001	SPRO-7	0.729 [9]	0.759 [9]	1.12 [9]	1.15 [9]	123.6** [9]

* - from DOESRAAD-SOT-001 showing 7 axially stacked segmented tubes/assembly
**-from DOESRAAD-SPRO-001 showing 6 axially stacked segmented tubes/assembly with 20.6" of fuel per tube

2.3.3.Heat Transfer:

Heat Source

The fuel is modeled as a heat source with the heat rate specified in Table 2-6. HWCTR and Segmented Oxide Tube (SOT) fuel rod heat generation rates were calculated from neutron flux and mass of U-235 using the reactor thermal power equation for heat generation. [28].

$$P = \phi \cdot \sigma \cdot E \cdot m\frac{N}{M}$$

P – Heat Rate of Fuel Rod
ϕ – Neutron Flux
σ – Microscopic Cross Section
E – Average Recoverable Energy Per Fission
m – Mass of U-235 in Fuel Rod
N – Avogadro's Number
M – Molar Mass of U-235

Microscopic cross section (585 barns), average recoverable energy per fission (200.7 MeV/fission), molar mass (235 g/mol), and Avogadro's Number (6.022E23 atoms/mol) are all properties of U-235 and are the same for all fuels described in the three HWCTR Appendix As: HWCTR-002, HWCTR-004, and SOT-001. The mass of U-235 in each fuel rod was determined from the corresponding Appendix A. The neutron flux for Test Fuel in the HWCTR (2.1E14 N/cm^2) also applies to all 3 fuel rods and was found in the IAEA directory on HWCTR [29]. Since there were 12 test fuel locations, this value was divided by 12 to determine the neutron flux for each fuel rod [28].

The maximum heat generation rate for the CVTR fuel was calculated from the maximum power level of 25.08 kw/ft and the length of fuel [3]. The heat generation rate for SRS P and R Production Reactors (SPRO) was calculated from the total reactor thermal power divided by the number of rods. This was done because individual data was not available and the power distribution within the core was nearly uniform [30]. EBWR fuel rod heat generation rates were found using Figure 5 in the memo by Vinson [7].

Table 2-6. Heat Generation Rates

Reactor	Appendix A	Heat Rate (W)
CVTR	DOESRAAD-CVTR-001	199545 [10]
EBWR	DOESRAAD-EBWR-002	6250 [5]
EBWR	DOESRAAD-EBWR-009	6726 [5]
EBWR	DOESRAAD-EBWR-004	22847 [5]
HWCTR	DOESRAAD-HWCTR-004	275600 [11, 28]
HWCTR	DOESRAAD-SOT-001, Rev. 2 SOT 1-3	179400 [28, 29]
HWCTR	DOESRAAD-SOT-001, Rev. 2 SOT 8-2	278000 [28, 29]
SRS-R	DOESRAAD-SPRO-001	556000 [9, 28]

Thermal Contact

The helium gap in the fuel rods is modeled as Thermal Contact with the "constriction conductance with interstitial gas contact model". This assumes that the fuel has expanded and is in contact with the cladding, but also accounts for the helium compressed between the fuel and cladding. This mode of heat transfer also accounts for radiative heat transfer from fuel to cladding. The thermal contact surface and gas properties were found in literature and are shown in Table 2-7 and Table 2-8.

Table 2-7. Thermal Contact Surface Properties

Reactor	Appendix A	Surface roughness, asperities average height (μm)	Surface roughness, asperities average slope*	Contact Pressure (MPa)	Microhardness** (GPa)
CVTR	DOESRAAD-CVTR-001	2.11 [31]	0.4	25 [32]	10 [33]
EBWR	DOESRAAD-EBWR-002	2.11 [31]	0.4	25 [32]	10 [33]
EBWR	DOESRAAD-EBWR-009	2.11 [31]	0.4	25 [32]	10 [33]
EBWR	DOESRAAD-EBWR-004	2.11 [31]	0.4	25 [32]	10 [33]
HWCTR	DOESRAAD-HWCTR-004	2.11 [31]	0.4	25 [32]	10 [33]
HWCTR	DOESRAAD-SOT-001, Rev. 2	2.11 [31]	0.4	25 [32]	10 [33]
SRS-R	DOESRAAD-SPRO-001	2.11 [31]	0.4	25 [32]	10 [33]

* - Default COMSOL value used
** - Maximum value from Fig. 4 of "Microhardness and Young's modulus of high burn-up UO_2 fuel" [33]

Table 2-8. Thermal Contact Gas Properties

Reactor	Appendix A	Gas Thermal Conductivity (W/(m*K))	Gas Pressure (MPa)	Gas thermal accommodation parameter	Gas Fluid Parameter*	Gas Particle Diameter (nm)	Surface Emissivity (upside and downside)
CVTR	DOESRAAD-CVTR-001	0.30 [34]	6 [35]	0.4 [36]	1.7	0.280 [37]	1,1
EBWR	DOESRAAD-EBWR-002	0.25 [34]	6 [35]	0.4 [36]	1.7	0.280 [37]	1,1
EBWR	DOESRAAD-EBWR-009	0.25 [34]	6 [35]	0.4 [36]	1.7	0.280 [37]	1,1
EBWR	DOESRAAD-EBWR-004	0.25 [34]	6 [35]	0.4 [36]	1.7	0.280 [37]	1,1
HWCTR	DOESRAAD-HWCTR-004	0.25 [34]	6 [35]	0.4 [36]	1.7	0.280 [37]	1,1
HWCTR	DOESRAAD-SOT-001, Rev. 2	0.25 [34]	6 [35]	0.4 [36]	1.7	0.280 [37]	1,1
SRS-R	DOESRAAD-SPRO-001	0.21 [34]	6 [35]	0.4 [36]	1.7	0.280 [37]	1,1

*Default COMSOL value

Heat Flux

The boiling water reactor fuel rods lose heat to the surrounding coolant through nucleate boiling on the surface of the cladding. A calculation was performed to determine if DNB occurred, which would result in higher fuel rod temperatures. DNB involves steam not breaking away from the surface, resulting in an insulating layer and higher cladding temperatures [15, 16]. Table 2-9 shows the COMSOL inputs for the nucleate boiling heat flux. Many of these inputs were standard for water and steam , but the liquid-surface combination factor was found in, “Introduction to Convective Boiling” [38]. EBWR-004 fuel was chosen for the CHF calculation because it is the BWR fuel that experienced the highest heat flux, therefore it would be the bounding case in determining if DNB occurred.[38].

Table 2-9 Nucleate Boiling Properties at 254°C

Reactor	Appendix A	Liquid	Vapor	Latent Heat of Vaporization [J/kg]	Liquid-Vapor Surface Tension [N/m]	Prandtl Number	Liquid-Surface Combination Factor
EBWR	DOESRAAD-EBWR-002	Water	Steam	1694700 [39]	0.025 [40]	1	0.013 [38]
EBWR	DOESRAAD-EBWR-009	Water	Steam	1694700 [39]	0.025 [40]	1	0.013 [38]
EBWR	DOESRAAD-EBWR-004	Water	Steam	1694700 [39]	0.025 [40]	1	0.013 [38]

The pressurized water reactor fuel rods lose heat to the surrounding coolant through convective heat transfer. The surrounding fluid pressure and temperature are used as inputs, along with fluid velocity. Velocity was either found directly from literature on the reactors or calculated from flow rate and channel area around or in the fuel rods.

Table 2-10 Convective Heat Loss Properties

Reactor	Appendix A	External Convection				Internal Convection			
		Cylinder Diameter [in]	Velocity, Fluid [m/s]	Absolute Pressure [atm]	External Temperature [°C]	Tube Diameter [in]	Velocity, fluid [m/s]	Absolute Pressure [atm]	External Temperature [°C]
CVTR	DOESRAAD-CVTR-001	0.4875 [10]	7.2 [3]	1	277.25 [3]	NA*	NA*	NA*	NA*
HWCTR	DOESRAAD-HWCTR-004	2.065 [11]	5.8 [29]	68 [29]	239 [29]	1.47 [11]	7.0 [29]	68 [29]	239 [29]
HWCTR	DOESRAAD-SOT-001, Rev. 2 SOT 1-3	2.065 [11]	5.8 [29]	68 [29]	239 [29]	1.47 [11]	7.0 [29]	68 [29]	239 [29]
	DOESRAAD-SOT-001, Rev. 2 SOT 8-2	3.6 [11]	5.8 [29]	68 [29]	239 [29]	2.98 [11]	7.0 [29]	68 [29]	239 [29]
SRS-R	DOESRAAD-SPRO-001	2.3 [9]	12.5 [41]	5 [psi] [41]	105 [41]	1.458 [9]	12.5 [41]	5 [psi] [41]	105 [41]

* CVTR fuel is rod shaped while HWCTR and SRS-R fuels are tube shaped

The Sieder-Tate correlation was used to calculate the heat transfer coefficient, which was an input for heat flux for the fuel rods from pressurized water reactors. [42]

$$\mathrm{Nu} = 0.027\,\mathrm{Re}^{4/5}\,\mathrm{Pr}^{1/3}\left(\frac{\mu}{\mu_w}\right)^{0.14}$$

where

$$\mathrm{Nu} = \frac{h d_h}{k}$$

$$\mathrm{Re} = \frac{d_h \rho v}{\mu}$$

$$\mathrm{Pr} = \frac{c_p \mu}{k}$$

where

Nu = Nusselt number
Re = Reynolds number
Pr = Prandtl number
d_h = hydraulic diameter = four times the flow area, divided by the wetted perimeter
ρ = fluid density
v = fluid velocity
μ = fluid viscosity
μ_w = fluid viscosity at the wall temperature
h = heat transfer coefficient

k = fluid thermal conductivity
c_p = fluid heat capacity

Table 2-11 Heat Transfer Coefficients for PWR Fuel

Reactor	Appendix A	External Heat Transfer Coefficient	Internal Heat Transfer Coefficient
		(W/m^2K)	(W/m^2K)
CVTR	DOESRAAD-CVTR-001	6.21E+04	NA
HWCTR	DOESRAAD-HWCTR-004	3.66E+04	4.72E+04
HWCTR	DOESRAAD-SOT-001, Rev. 2 SOT 1-3	3.66E+04	4.09E+04
	DOESRAAD-SOT-001, Rev. 2 SOT 8-2	4.47E+04	4.09E+04
SRS-R	DOESRAAD-SPRO-001	3.26E+04	5.57E+04

3. Results

The calculated temperatures for all the analyzed fuels are shown in Table 3-1. The temperatures are given for each of the components of the fuel rods: Fuel, Inner Cladding, and Outer Cladding. Inner cladding refers to the boundary between fuel and cladding. Outer cladding refers to the surface of the cladding. For tubes, the maximum temperature is shown for either the interior or exterior cladding, whichever experienced the higher temperature. The rods from the CVTR may have experienced inner cladding temperatures above 350 °C. Temperature plots of all modeled fuel rods are shown in Appendix 1.

Table 3-1. Fuel Rod Component Temperatures

Reactor	Appendix A	Maximum Fuel Temp (°C)	Maximum Inner Cladding (°C)	Maximum Outer Cladding (°C)
CVTR	**DOESRAAD-CVTR-001**	**2729.0**	**447.1**	**311.6**
EBWR	**DOESRAAD-EBWR-002**	**364.6**	**267.4**	**258.3**
EBWR	**DOESRAAD-EBWR-009**	**372.5**	**267.7**	**258.4**
EBWR	**DOESRAAD-EBWR-004**	**652.4**	**296.5**	**258.9**
HWCTR	**DOESRAAD-HWCTR-004**	**397.9**	**273.0**	**247.8**
HWCTR	**DOESRAAD-SOT-001, REV. 2: SOT 1-3**	**386.2**	**271.4**	**247.5**
HWCTR	**DOESRAAD-SOT-001, REV. 2: SOT 8-2**	**391.1**	**266.1**	**246.7**
SRS-R	**DOESRAAD-SPRO-001**	**491.1**	**164.9**	**121.7**

4. Conclusions

This report outlines the thermal modeling approach used to determine maximum cladding temperature of Zircaloy-cladded UO_2 fuel in NASNF Campaign 1 to aid in the determination of potential UZr intermetallic formation in these assemblies. The CVTR assemblies were determined to have most likely experienced temperatures higher than the 350 °C conservative temperature threshold for intermetallic UZr formation. This does not necessarily mean that intermetallic UZr compound is present but provides a conservative indicator that it could have formed. The calculations for the other fuel rods all result in cladding temperatures below 350 °C.

5. References

[1] M. W. Mallett, J. W. Droege, A. F. Gerds, and W. A. Lemmon, "Zirconium-Uranium Dioxide Reaction," Battelle Memorial Institute, BMI-1210, 1957.

[2] T. T. Truong and R. A. Pierce, "Task Technical and Quality Assurance Plan for Evaluating Uranium-Zirconium Intermetallic Formation in Zircaloy Clad Uranium Oxide Fuels," SRNL-RP-2023-00055, 2023.

[3] M. G. Balfour, "Design, Fabrication and Operation of the CVTR High-Power, High-Burnup Test Assemblies," Westinghouse Electric Corperation, Atomic Power Divisions, Madison, PA, CVNA-274, 1967.

[4] T. C. Andes, "DOESRAAD-EBWR-002," United States Department of Energy, Savannah River Site (SRS), 8 October 2001 2001.

[5] D. Koehne-Singer, "DOESRAAD-EBWR-004," United States Department of Energy, Savannah River Site (SRS), 25 March 2002 2002.

[6] D. P. Eisele, "DOESRAAD-EBWR-009," United States Department of Energy, Savannah River Site (SRS), 4 November 2002 2002.

[7] D. W. Vinson, "Evaluation of the Isotopic and Decay Heat Characteristics of Spent Nuclear Fuel Discharged from the Experimental Boiling Water Reactor," SRT-MTS-2002-20003, 2002.

[8] J. Thomas, "DOESRAAD-SOT-001, REV. 2," United States Department of Energy, Savannah River Site (SRS), 1 October 2002 2002.

[9] J. Thomas, "DOESRAAD-SPRO-001," United States Department of Energy, Savannah River Site (SRS), 18 June 2002 2002.

[10] D. P. Eisele, "DOESRAAD-CVTR-001," United States Department of Energy, Savannah River Site (SRS), 23 September 2002 2002.

[11] T. C. Andes, "DOESRAAD-HWCTR-004," United States Department of Energy, Savannah River Site (SRS), 9 January 2001 2001.

[12] "COMSOL Multiphysics Software Test Documentation," Savannah River Site (SRS), B-STP-A-00041, Rev. 3.

[13] "Software Evaluation Package (SEP) for COMSOL Multiphysics," Savannah River Site (SRS), B-SEP-A-00002, Rev 4.

[14] "Software Quality Assurance Plan for COMSOL Multiphysics," Savannah River Site (SRS), B-SQP-A-00057, Rev. 4.

[15] F. E. Dunn, E. H. Wilson, E. E. Feldman, K. Sun, and C. Wang, "Evaluation of a Uranium Zirconium Zirconium Hydride Fuel Rod Option For Conversion of the MIT Research Reactor (MITR) From Highly-Enririched Uranium to Low-Enriched Uranium," *Nuclear Engineering and Design,* vol. 317, pp. 15-21, 2017. [Online]. Available: https://doi.org/10.1016/j.nucengdes.2017.02.034.

[16] D. C. Groeneveld, "Critical Heat Flux Data Used to Generate the 2006 Groeneveld Lookup Tables," U. S. Nucelar Regulatory Commission, Thermalhydraulics Consultans Inc., NUREG/KM-0011, 2019. [Online]. Available: https://www.nrc.gov/docs/ML1902/ML19029B306.pdf

[17] M. Murabayashi, "Thermal Conductivity and Heat Capacity of Zircaloy-2, −4 and Unalloyed Zirconium," *Journal of Nuclear Science and Technology,* vol. 12, no. 10, pp. 661-662, 1965, doi: 10.1080/18811248.1975.9733170.

[18] *Properties and Selection: Nonferrous Alloys and Special-Purpose Materials.* . ASM International, 1992.

[19] "Thermophysical Properties of Materials for Nuclear Engineering: A Tutorial and Collection of Data," International Atomic Energy Agency, Vienna, Austria, 2008. [Online]. Available: https://www-pub.iaea.org/MTCD/Publications/PDF/IAEA-THPH_web.pdf

[20] T. Matsumoto and M. Kato. "Thermal and Mechanical Properties of UO2 and PUO2." NEA/NSC/R(2015)2, https://inis.iaea.org/collection/NCLCollectionStore/_Public/47/093/47093736.pdf (accessed 2023).

[21] H. Ziebland and J. T. A. Burton, "The Thermal Conductivity of Heavy Water between 75 ° and 260°C at Pressures up to 300 atm," *International Journal of Heat and Mass Transfer,* vol. 1, pp. 242-254, 1960. [Online]. Available: https://doi.org/10.1016/0017-9310(60)90001-6.

[22] G. Ulrych, "Properties of Liquid Heavy Water," *Heat Exchanger Design Handbook, Multimedia Edition*. [Online]. Available: https://hedhme.com/content_map/?link_id=22146&article_id=532.

[23] P. Z. Rosta. "Specifc Heat and Enthalpy of Liquid Heavy Water." Atomic Energy of Canada Limited, IPEN. https://www.ipen.br/biblioteca/rel/R30758.pdf (accessed 2023).

[24] P. G. Hill, R. D. MacMillan, and V. Lee, "Tables of Thermodynamic Properties of Heavy Water in S.I. Units," Atomic Energy of Canada Limited, IAEA.org, 1981. [Online]. Available: https://inis.iaea.org/collection/NCLCollectionStore/_Public/14/730/14730979.pdf?r=1

[25] B. L. Neindre, P. Bury, R. Tufeu, and B. Vodar, "Thermal Conductivity Coefficients of Water and Heavy Water in the Liquid State up to 370. Degree. C," *Journal of Chemical & Engineering Data,* vol. 21, pp. 265-274, 1976. [Online]. Available: https://doi.org/10.1021/je60070a018.

[26] "Heavy Water, Deuterium Oxide, D2O." MatWeb. https://www.matweb.com/search/datasheettext.aspx?matguid=5f6bec9d37a84a77bcf295bf3653ac58 (accessed 2023).

[27] R. Hardy and R. L. Cottington, "Viscosity of Deuterium Oxide and Water in the Range 5 to 125 C," *Journal of Research of the National Bureau of Standards,* 1949. [Online]. Available: https://nvlpubs.nist.gov/nistpubs/jres/42/jresv42n6p573_A1b.pdf.

[28] "Heat Generation in Nuclear Reactors: Characteristics." Nuclear Power. https://www.nuclear-power.com/nuclear-engineering/heat-transfer/heat-generation/ (accessed 2023).

[29] "IAEA Directory on HWCTR," USA, 1962.

[30] "Evaluation of Activation Products in Remaining R- and P-Reactor Structures," Savannah River National Laboratory SRNL-STI-2010-00545, 2010.

[31] M. Said, "Quantifying Surface Roughness on UO2 Fuel Pellets Using Optical Techniques," *Forensic Science International,* vol. 316, art. 110470, 2020. [Online]. Available: https://doi.org/10.1016/j.forsciint.2020.110470.

[32] D. Carpenter, "Comparison of Pellet-Cladding Mechanical Interaction for Zircaloy and Silicon Carbide Clad Fuel Rods in Pressurized Water Reactors," MIT, 2006. [Online]. Available: https://ocw.mit.edu/courses/22-314j-structural-mechanics-in-nuclear-power-technology-fall-2006/736d80e4e6bf84e40c9dc3cff49be3fb_carpenter.pdf

[33] F. Cappia *et al.*, "Microhardness and Young's Modulus of High Burn-up UO2 Fuel.," *Journal of Nuclear Materials,* vol. 479, pp. 447-454, 2016. [Online]. Available: https://doi.org/10.1016/j.jnucmat.2016.07.015.

[34] A. Purohit and J. R. Moszynaki, "Thermal conductivity of the helium-argon system. ," Argonne National Laboratory, Argonne, Illinois, ANL-79-3, 1979. [Online]. Available: https://www.osti.gov/biblio/6297285

[35] "End-of-Life Rod Internal Pressures in Spent Pressurized Water Reactor Fuel." EPRI. https://www.epri.com/research/products/000000003002001949 (accessed 2023).

[36] W. Trott, R. Merle, J. Daniel, J. N. Castaneda, J. R. Torczynski, and M. A. Gallis, "Experimental Measurements of Thermal Accommodation Coefficients for Microscale Gas-Phase Heat Transfer," Sandia National Laboratory, Albuquerque, New Mexico, SAND2006-6432C, 2006, vol. 2023. [Online]. Available: https://www.osti.gov/servlets/purl/1264272

[37] "PubChem Element Summary for Atomic Number 2, Helium." PubChem. https://pubchem.ncbi.nlm.nih.gov/element/Helium (accessed 2023).

[38] J. G. Collier, *Introduction to Convective Boiling. Convective Boiling and Condensation*. Maidenhead: McGraw Hill, 1972.

[39] "Water - Heat of Vaporization vs. Temperature [489 F]." Engineering ToolBox. https://www.engineeringtoolbox.com/water-properties-d_1573.html (accessed 2023).

[40] N. B. Vargaftik, B. N. Volkov, and L. D. Voljak, "International Tables of the Surface Tension of Water," *Journal of Physical and Chemical Reference Data,* vol. 12, no. 3, 1983, pp. 817-820. [Online]. Available: https://srd.nist.gov/JPCRD/jpcrd231.pdf.

[41] "R Reactor," Savannah River Plant, SRO-00104 (UCNI), 1964.

[42] T. L. Bergman, A. S. Levine, F. P. Incropera, and D. P. DeWitt, *Fundamentals of Heat and Mass Transfer, 7th ed*. New York: John Wiley & Sons, 2011.

[43] B. J. Toppel, P. J. V. Jr., and E. A. Wimunc, "Safety Analysis Associated with the Plutonium Recycle Experiment in EBWR," Argonne National Laboratory ANL6841, 1964.

[44] M. J. Moran, H. N. Shapiro, D. D. Boettner, and M. B. Bailey, *Fundamentals of Engineering Thermodynamics 7th ed.*, New York: John Wiley & Sons, Inc., 2011.

6. Appendix 1. Temperature Profiles for Reactor Assemblies

Figure 6-1. CVTR-001 Temperature Plot

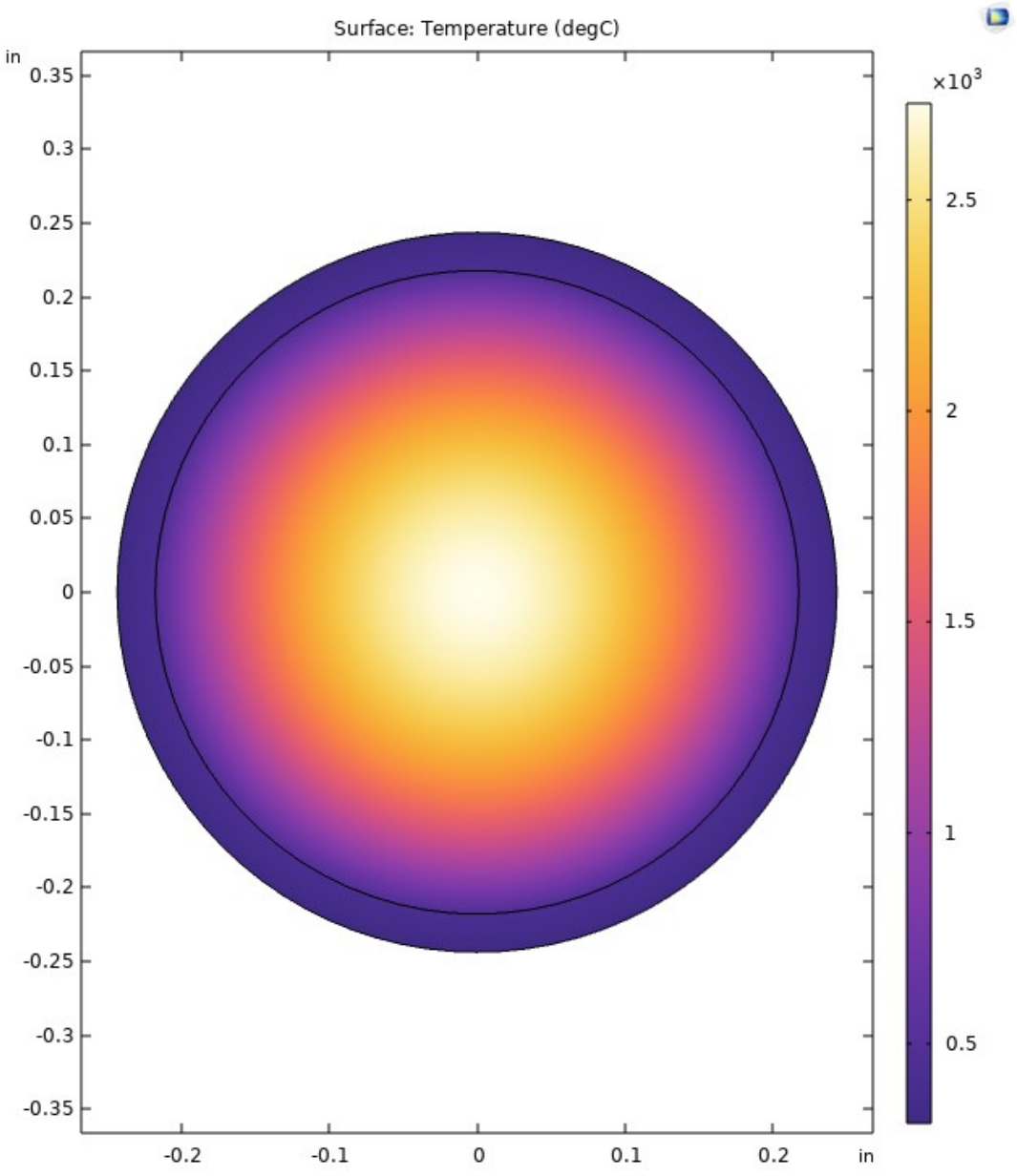

Figure 6-2. EBWR-002 Temperature Plot

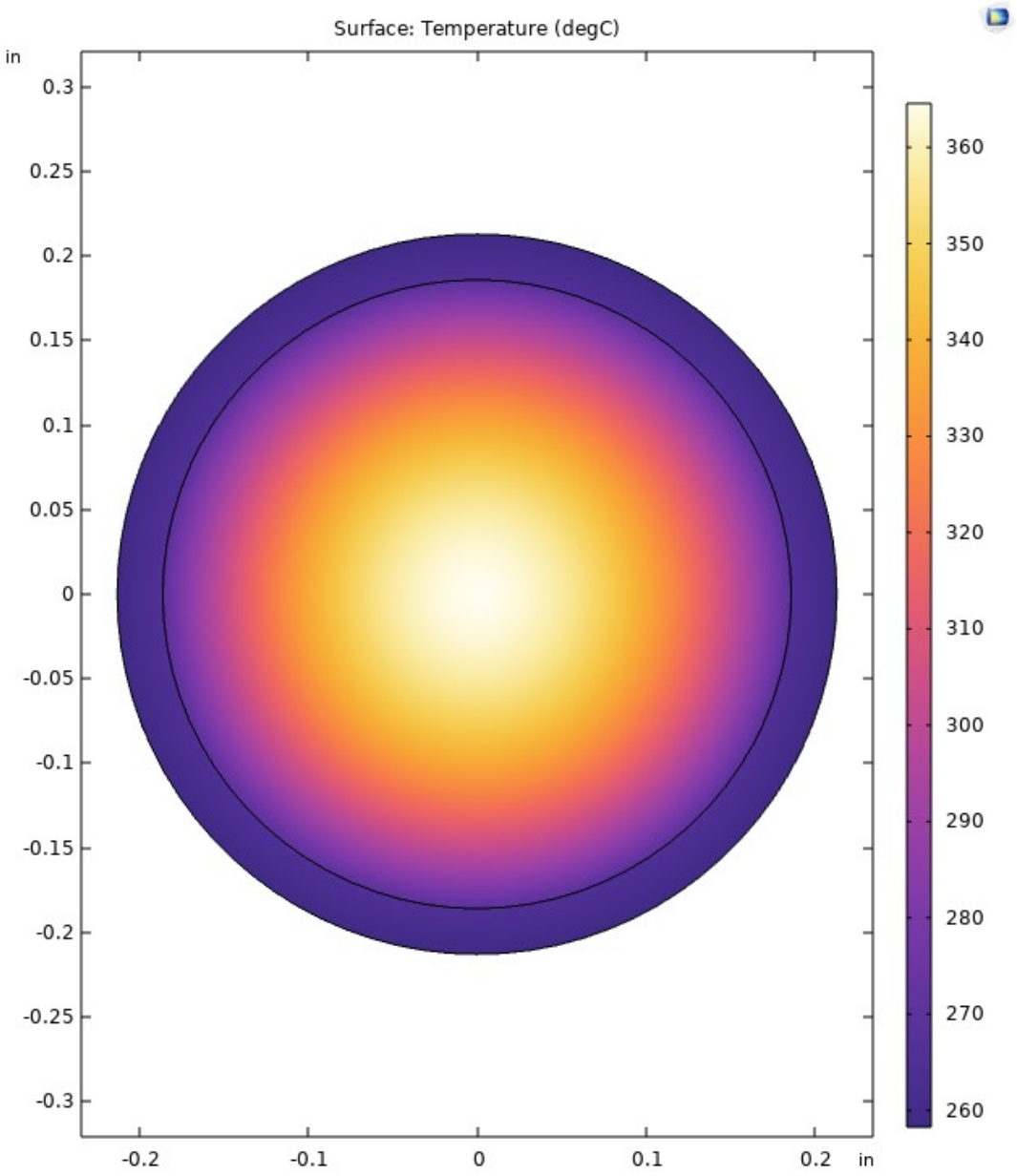

Figure 6-3. EBWR-009 Temperature Plot

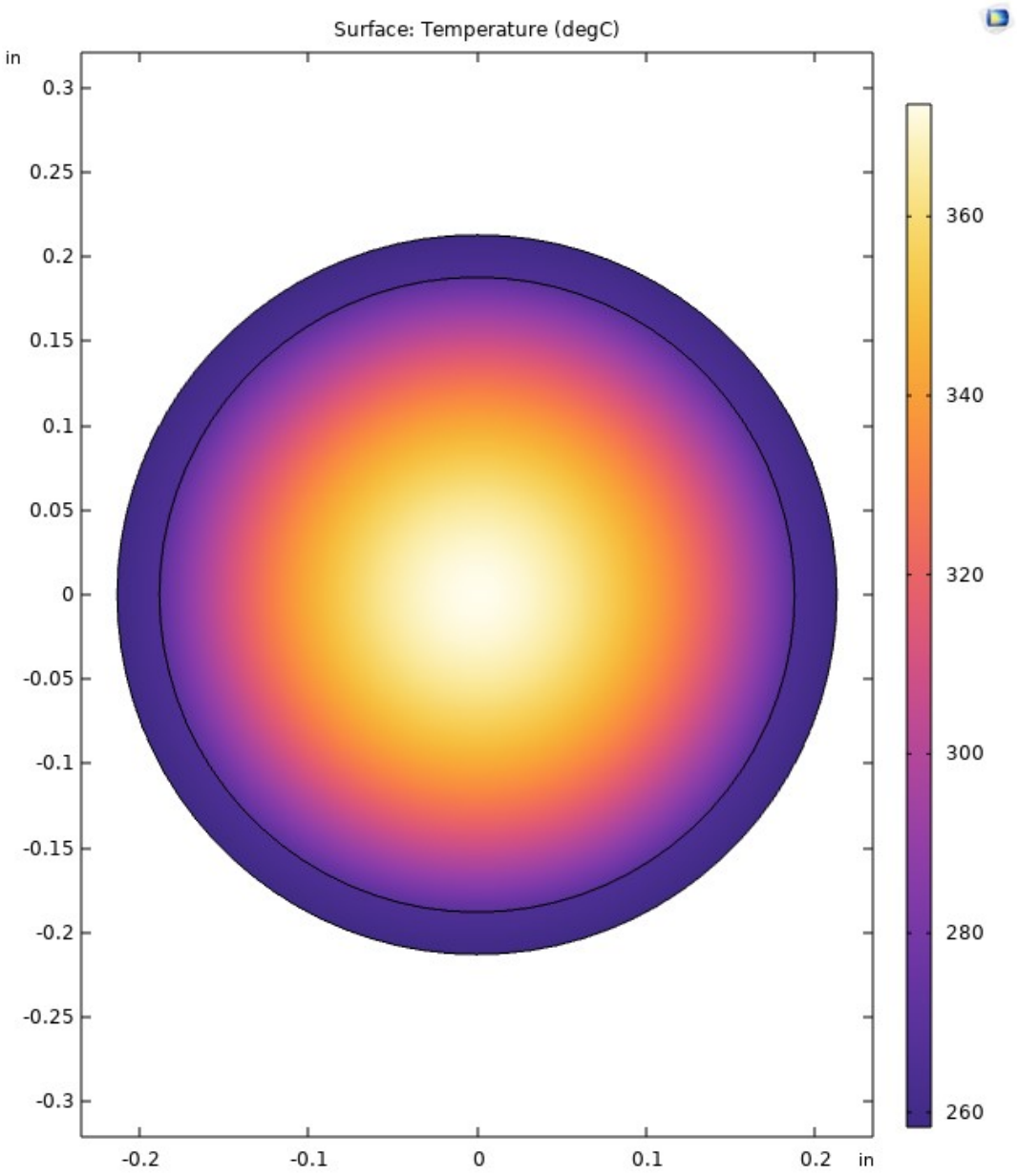

Figure 6-4. EBWR-004 Temperature Plot

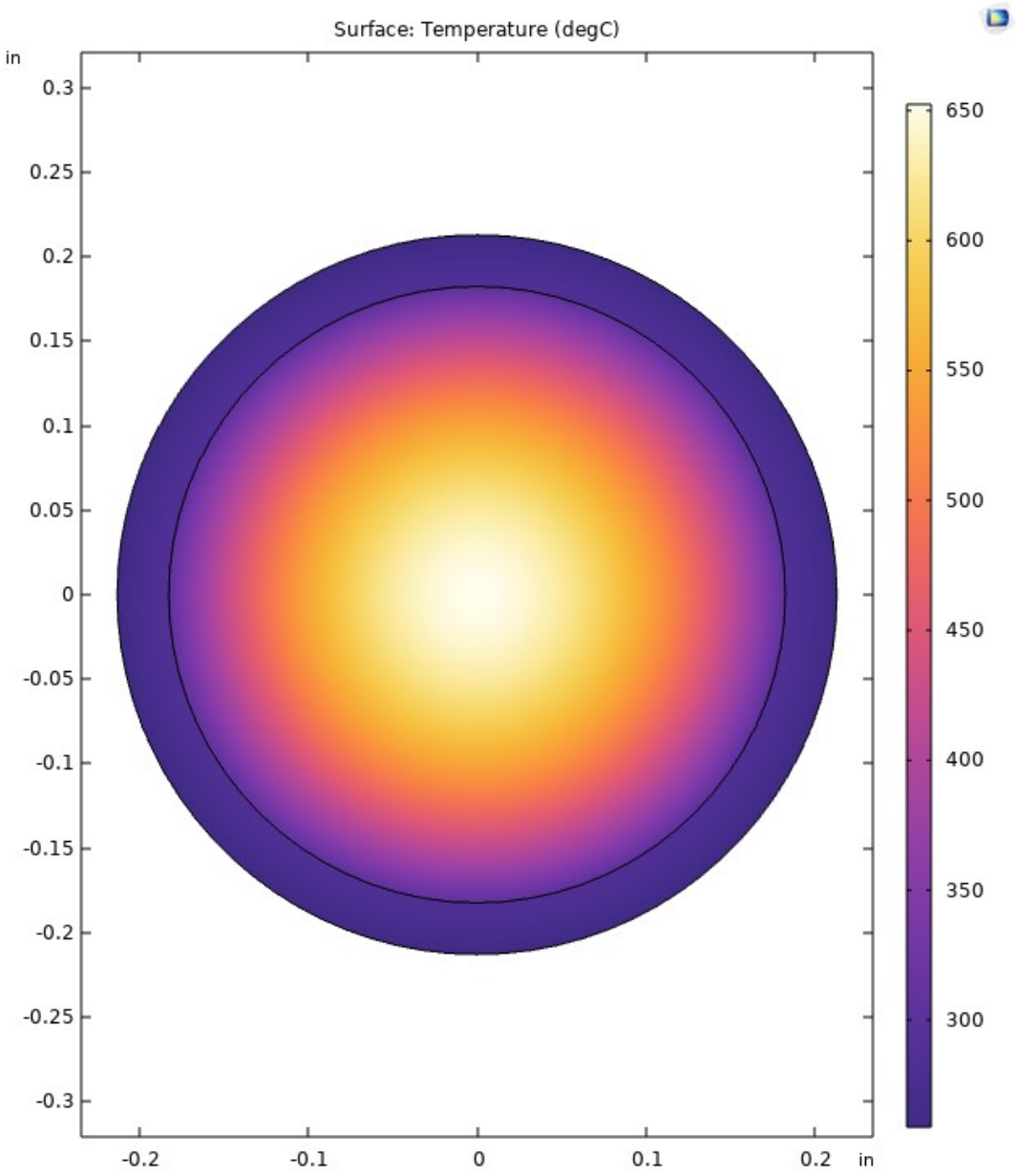

Figure 6-5. HWCTR-004 Temperature Plot

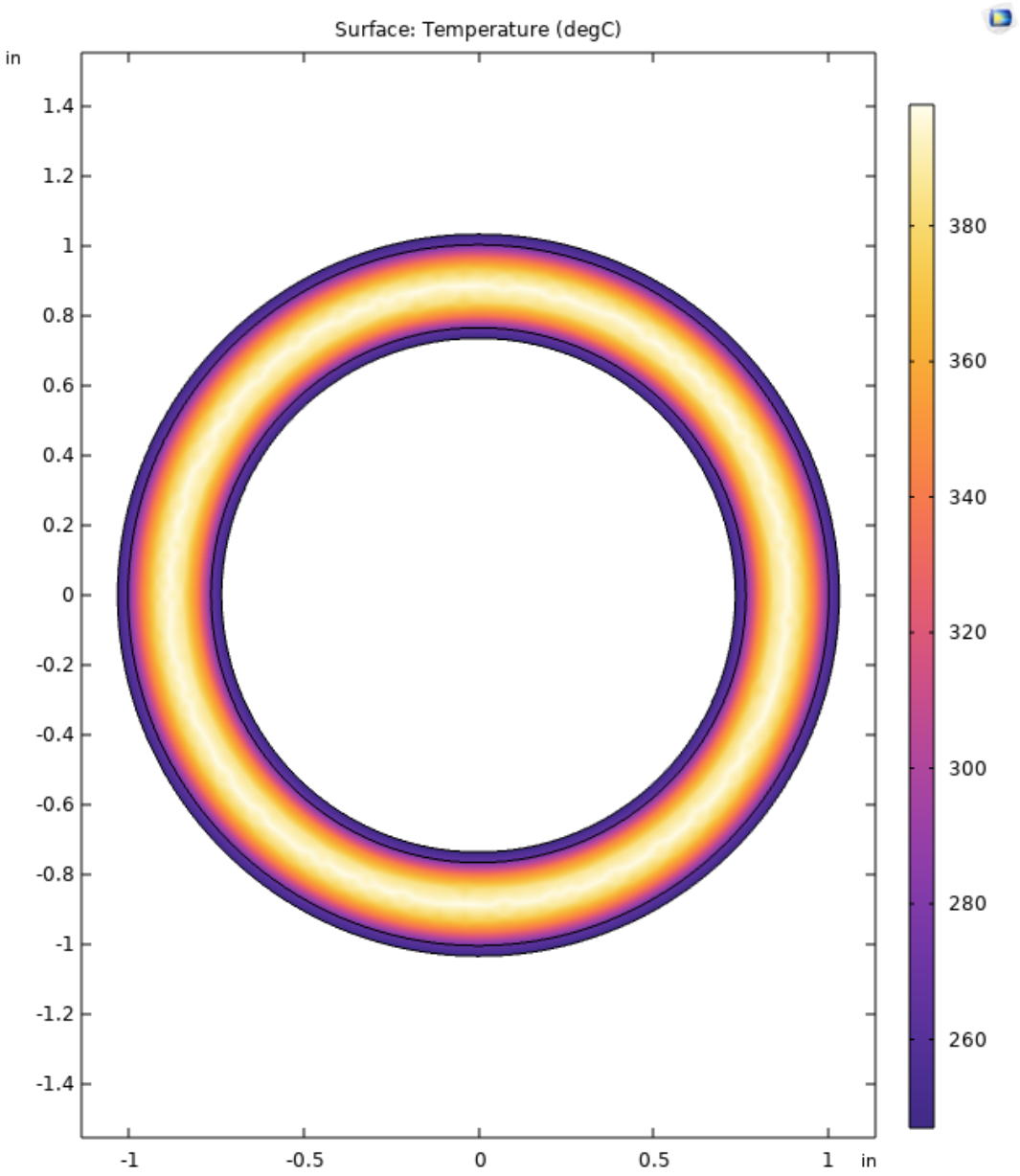

Figure 6-6. SOT 1-3 Temperature Plot

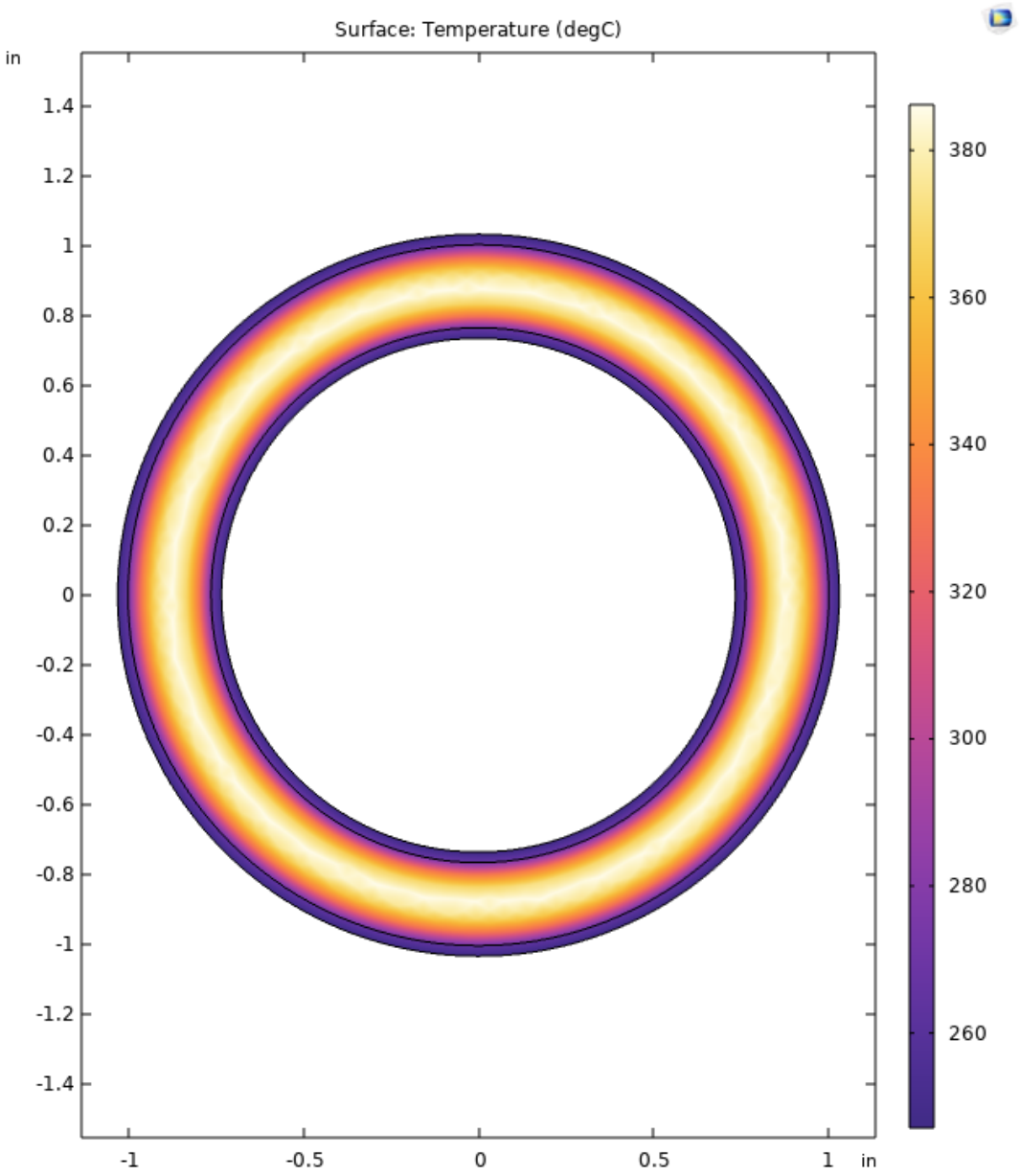

Figure 6-7. SOT 8-2 Temperature Plot

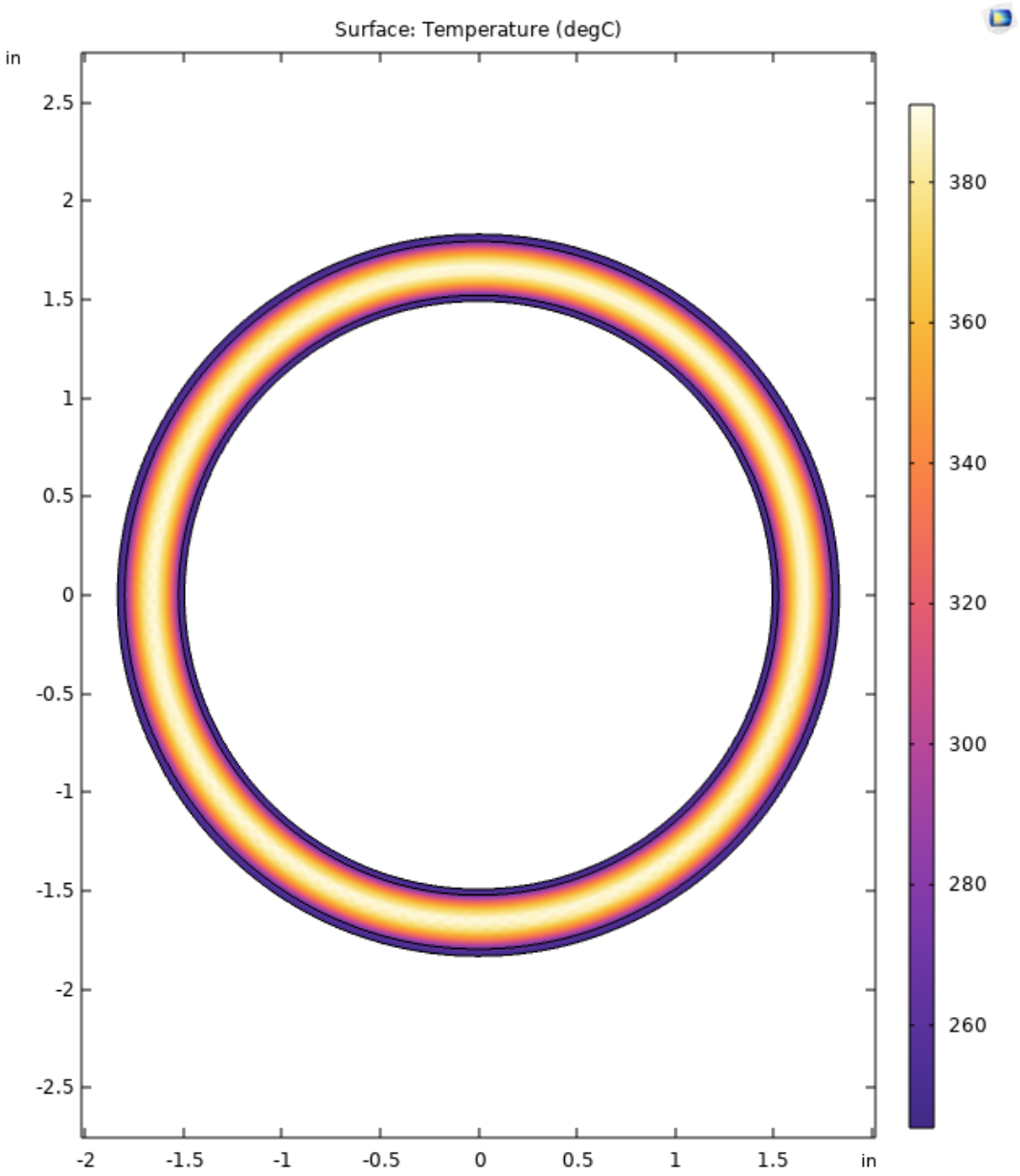

Figure 6-8. SPRO-001 Temperature Plot

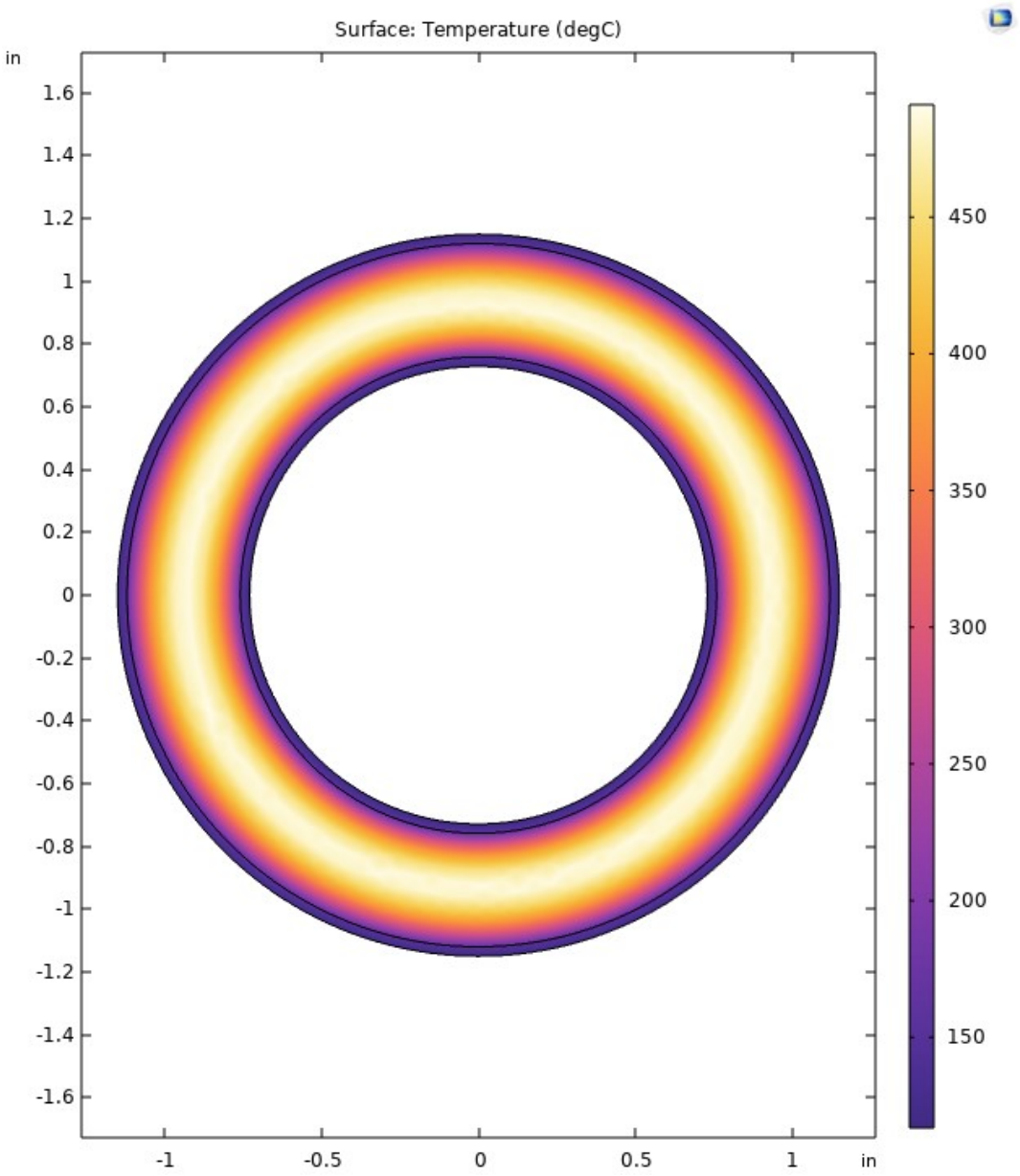

7. Appendix 2. Critical Heat Flux Analysis for EBWR-004

Calculations for critical heat flux (CHF) are shown below. Reference [15] describes these equations and how to apply them. Several of the values used were found in literature [43, 44]. These values are noted where they are used.

CHF Calculation for EBWR-004 [15]

P=600 psi **[43]**

$X := .0235$ Steam Quality **[43]**

$chf := 6600 \frac{kW}{m^2}$ interpolated from lookup tables **[16]**
The following correction factors are applied: K1, K2, K3, K4 to account for variations from an 8mm tube

$v := 3.75 \frac{ft}{s}$ **[43]**

$\rho := 49 \frac{lb}{ft^3}$

$G_1 := \rho \cdot v = 897.146 \frac{kg}{m^2 \cdot s}$

$G := 897.146 \frac{kg}{m^2 \cdot s}$

$D := 10.82 \cdot \left[\frac{4}{3.14} \cdot \left(\frac{14.45}{10.82} \right)^2 - 1 \right] = 13.763$ mm hydraulic diameter: rectangular lattice with dimensions shown in Figure 5 in **[43]**

$n := .312$ **[15]**

$K_1 := \left(\frac{8}{D} \right)^n = 0.844$

$K_2 := .8 \cdot e^{\left(-.5 \cdot X^{.333} \right)} = 0.693$

$K := .37$ (K is the pressure loss coefficient. information was not available for this rod bundle, but 0.37 was used in a similar calculation)

$A := 1.5 \cdot K^{.5} \cdot (.001 \cdot G)^2$

$B := .1$

$L_{sp} := 610$ mm **[43]**

$K_3 := 1 + A \cdot e^{\left(-B \cdot \frac{L_{sp}}{D} \right)} = 1.011$

$L := 1219.2 \ mm$ heated length **[4]**

$\rho_f := 782.68 \ \frac{kg}{m^3}$ **[44]**

$\rho_g := 21.33$

$$\alpha := X\cdot\left[\frac{\rho_f}{X\cdot\rho_f + (1 - X)\cdot\rho_g}\right] = 0.469$$

$$K_4 := e^{\left[\left(\frac{D}{L}\right)\cdot\left(e^{2\cdot\alpha}\right)\right]} = 1.029$$

$$CHF := chf\cdot K_1\cdot K_2\cdot K_3\cdot K_4 = 4.017 \times 10^6 \ \frac{kg}{s^3}$$ **4017 kW/m^2**

$Q_{actual} := 551.5 \ \frac{kW}{m^2}$ Actual heat flux is well below CHF. Calculated from heat generation rate divided by surface area of fuel rod

Distribution:

T. Armstead, 704-2H
A. C. Barnes, 704-2H
W. F. Bates, 773-A
S. J. Brown, 221-H
K. P. Burrows, 704-2H
W. G. Dyer, 704-2H
J. P. Folk, 723-A
J. Gogolski, 773-A
D. T. Herman, 735-11A
A. M. Hudlow, 704-2H
J. C. Kinney, 730-A
J. E. Laurinat, 773-41A
T. A. Nance, 730-A
J. L. Nguyen, 221-H
F. M. Pennebaker, 773-A
M. H. Phillips, 730-A
R. A. Pierce, 773-A
C. D. Skinner, 723-A
W. A. Stafford, 723-A
J. E. Therrell, 703-H
T. T. Truong, 773-41A
N. A. Vinci, 221-H
H. M. Vu, 704-2H
B. J. Wiedenman, 773-42A